NANO: Brief Reports and Reviews
Vol. 11, No. 3 (2016) 1650027 (12 pages)

DOI: 10.1142/S1793292016500272

SMALL-ANGLE X-RAY SCATTERING STUDY ON PVA/Fe_3O_4 MAGNETIC HYDROGELS

Sunaryono* and Ahmad Taufiq
Department of Physics, Faculty of Mathematics and Natural Sciences, Institut Teknologi Sepuluh Nopember, Kampus ITS Sukolilo, Surabaya 60111, Indonesia
Department of Physics, Faculty of Mathematics and Natural Sciences, Universitas Negeri Malang, Malang 65145, Indonesia
**sunaryono.fmipa@um.ac.id*

Edy Giri Rahman Putra
Center for Science and Technology of Advanced Materials, National Nuclear Energy Agency of Indonesia, Kawasan Puspiptek Serpong, Tangerang15134, Indonesia

Atsushi Okazawa
Department of Basic Science, Graduate School of Arts and Sciences, The University of Tokyo, Komaba 3-8-1, Meguro-ku, Tokyo, 153-8902, Japan

Isao Watanabe
Advanced Meson Laboratory, Nishina Accelerator Based Science Center, RIKEN, 2-1 Hirosawa, Wako-shi, Saitama, 351-0198, Japan
nabedon@riken.jp

Norimichi Kojima
Toyota Physical and Chemical Research Institute, Yokomichi 41-1, Nagakute, Aichi 480-1192, Japan
kojima@toyotariken.jp

Supagorn Rugmai+ and Siriwat Soontaranon++
Synchrotron Light Research Institute, 111 University Venue, Muang District, Nakhon Ratchasima 30000, Thailand

Mohammad Zainuri▲, Triwikantoro☼, Suminar Pratapaπ, and Darminto*
Department of Physics, Faculty of Mathematics and Natural Sciences, Institut Teknologi Sepuluh Nopember, Kampus ITS Sukolilo, Surabaya 60111, Indonesia

Received 28 August 2015
Accepted 05 November 2015
Published 07 January 2016

A synchrotron small-angle X-ray scattering (SAXS) study on PVA/Fe_3O_4 magnetic hydrogels has been performed to investigate the effect of clustering on their magnetic properties. The hydrogels were prepared through freezing-thawing (F-T) processes. The structure, morphology and magnetic properties of magnetite (Fe_3O_4) nanoparticles were investigated using X-ray diffractometry (XRD), transmission electron microscopy (TEM) and a superconducting quantum interference device

*Corresponding author

(SQUID) magnetometer, respectively. In this study, SAXS data were used to reveal the structural dimensions of the magnetite and its distribution in the polymer-rich PVA and magnetic hydrogels. As calculated using the Beaucage and Teubner-Strey models, the average of the structural dimensions of the PVA hydrogels was 3.9 nm (crystallites), while the average distance between crystallites was approximately 18 nm. Further analysis by applying a two-lognormal distribution showed that the magnetite nanoparticles comprised secondary particles with a diameter of 9.6 nm that were structured by primary particles (~ 3.2 nm). A two-lognormal distribution function has also been used in describing the size distributions of magnetite nanoparticles in magnetic hydrogels. The clusters of magnetite nanoparticles in the magnetic hydrogels are significantly reduced from 30.4 to 12.8 nm with decreasing concentration of the nanoparticles magnetite from 15 to 1 wt%. The saturation magnetization values of the magnetite nanoparticles, the 15% and 1% magnetic hydrogels were 34.67, 6.52, and 0.37 emu/g, respectively.

Keywords: SAXS; magnetic hydrogel; primary particle; secondary particle; cluster.

1. Introduction

Polyvinyl alcohol (PVA) is a synthetic polymer that is non-toxic, exhibits physical ability and biocompatibility, and is widely applied in biomedical applications[1] and drug delivery systems.[2] PVA hydrogel is one example of a flexible material that is arranged by the networking structure of polymer chains. The networking structure can be formed by a physical cross-linked polymer network, which is henceforth referred to as a physical gel, and a chemical cross-linked polymer network, which is henceforth called a chemical gel. Physical gels are formed by ionic interactions, hydrophobic interactions, van der Waals forces, and hydrogen bonds, while chemical gels are formed by covalent bonds.[3] PVA hydrogels can be produced by various methods, such as the γ-irradiation process, crosslinking agent process, and freezing-thawing cycles.

Magnetic hydrogel, a responsive magnetic gel combining the elastic properties of PVA hydrogel and the magnetic properties of magnetite (Fe_3O_4),[4] represents a new class of composite materials that exhibits potential uses in medical, industrial and technological applications. Several potential applications were reported by previous researchers, such as magneto-thermal for hyperthermia in cancer therapy,[5] fabrication of core-shell structured magnetite nanoparticles and gold with polydopamine for biomedical applications,[6] tunable elastic for industry as vibration absorbers,[7] the fabrication of magnetite nanoclusters for magneto-motive ultrasound imaging,[8] soft ferrogel with multi-responsive particles for a catalyst and drug delivery,[9] magneto-rheological (MR) elastomers for anti-friction and control mechanical components as novel force sensors.[10] In our previous report,[11] magnetic hydrogels with a filler of magnetite nanoparticles from a local iron sand have been successfully prepared. Based on the magneto-elasticity characterization, the threshold magnetic field decreased with increasing magnetite concentration. The mechanical displacement-applied current patterns of the magnetic hydrogels had a tendency to form a hysteresis curve as an impact of the magnetite nanoparticles. Furthermore, Ramanujan *et al.*[12] also developed magnetic hydrogels that were sensitive to an external magnetic field. Their performance was interesting because they were dimensionally responsive, lightweight, controllable and flexible, as well as able to undergo a cyclic deformation, making them potentially useful as an artificial muscle or a soft actuator.[12]

Several researchers have also investigated the mechanical and magnetic properties of magnetic hydrogels that were obtained by mixing PVA hydrogels and magnetite filler via a freezing-thawing process. As found by Liu *et al.*[4], magnetic hydrogels with a composition of 17-34% magnetite and 10% PVA that were prepared through an F-T process (16 h of freezing and 5 h of thawing), repeated 3 times, showed the optimum magnetic-response properties. The saturation magnetization for the magnetic hydrogel with a PVA matrix of 5 wt% and magnetite (5-10 nm in diameter) filler of 17 wt% was 10.84 emu/g. Using a similar F-T process with 16 h of freezing and 8 h of thawing, Resendiz-Hernandez *et al.*[13] reported that the saturation magnetization value of magnetic hydrogels comprising PVA (2 g), dimethyl sulfoxide (30 ml), and magnetite (2 g) was 0.6 emu/g. Meanwhile, a value of saturation magnetization of magnetic hydrogels with a magnetite filler of 6 wt% of

approximately 3.64 emu/g was reported by Gonzalez *et al.*.[14] However, the time for the freezing-thawing preparation processes reported so far were relatively long, i.e. > 3 hours. Therefore, the preparation of magnetic hydrogels with less processing time with attained magnetic saturations is imperative.

Despite the relatively massive knowledgebase on the magnetic behavior of ferrogels, only a few references are available on the study of their structural dynamics. To investigate the structural and dynamical properties of polymer (hydrogels and magnetic hydrogels), magnetite nanoparticles in magnetic hydrogels, liquid crystals, micellar solutions, proteins, membranes, enzymes, etc., an advanced tool such as small-angle scattering (SAS), either by neutron (SANS) or X-ray (SAXS), is required. Puspitasari *et al.*[15] reported that the structural organization of PVA hydrogels was conducted successfully by using the SANS technique. They confirmed that PVA hydrogels consist of polymer crystallite with a radius of approximately 2.8-3.3 nm and an average distance between crystallites of 15-17.5 nm. A similar result was also reported that the structures of isotropic PVA hydrogels composed in the polymer-rich phase have structural dimensions of 3 nm and are distributed with an average distance of 19 nm.[16] Hernandez *et al.*[17] reported that the primary particles of magnetite nanoparticles in polymer gels investigated by using SAXS presenting 6.6 to 10.0 nm. Meanwhile, Priola *et al.*[18] showed by using SAXS analysis that the distribution of magnetite nanoparticles in magnetic hydrogels with a matrix of poly(acrylamide-co-hydroxyethyl-acrylate) cross-linked using poly-ethylene-glycol-diacrylate formed a bimodal magnetite nanoparticle size distribution, namely, 1.5-2.0 nm and 3.0-3.5 nm. Moscoso-Londono *et al.*[19] revealed that the structural dimensions of magnetic hydrogels obtained by using the freezing-thawing process were calculated by using the Guinier formula. They showed that the radius of gyrations of magnetite nanoparticles inside the PVA hydrogels, which contained non-coated magnetite nanoparticles, is (11.0 ± 0.6) nm. Furthermore, Hernandez *et al.*[20] have successfully investigated the primary particles and aggregations of the magnetite nanoparticles using the unified fitting model. However, in order to have a better understanding in studying the hierarchical structure of magnetite nanoparticles and hydrogels magnetic such as primary particles, secondary particles, and also their clusters, we propose another model by using two-lognormal distribution and fractal models as global fitting.

In this paper, we report the size distribution of primary and secondary particles as well as clusters of magnetite nanoparticles in magnetic hydrogels by using the synchrotron radiation SAXS technique with global fitting analysis data. PVA and magnetic hydrogels were prepared by an optimized physical crosslink of the freezing-thawing (F-T) process. The distribution of magnetite nanoparticles in the magnetic hydrogels and its associated saturation magnetization were also examined.

2. Experimental Method

2.1. Preparation of Magnetite Nanoparticles

The magnetite source was iron sand taken from the Tulungagung District, Indonesia. Hydrochloric acid (HCl) with a molarity of 12.063 M (Sigma Aldrich) was used as the solvent solution, while ammonium hydroxide (NH_4OH) with a molarity of 6.5 M (Sigma Aldrich) was used as the precipitating agent, and distilled water was used to wash the precipitate during synthesis of the magnetite nanoparticles. The magnetite nanoparticles were prepared by a co-precipitation method following the previous works.[11,21-23] The more detail of preparation procedure of magnetite nanoparticles is described as the following steps. Firstly, the iron sand which is extracted by using a permanent magnet, with a certain composition, was dissolved in 29 mL of HCl solution for 20 minutes with a magnetic stirrer at 1000 rpm and room temperature. Secondly, the dissolved sand was mixed with droplets of NH_4OH for 30 min by using a magnetic stirrer at 1000 rpm and room temperature until a complete precipitation, indicated with the color of the solution changed from brown to black as the indication the forming of magnetite nanoparticles, was reached. Finally, the mixture of precipitate and solution was filtered and then washed by repeated cycles for 5 times with distilled water to obtain the precipitates of magnetite nanoparticles. The precipitate was dried under vacuum at 100 °C for 1 h prior to characterization.

2.2. Fabrication of PVA Hydrogels

The PVA polymeric powder (Merck Schuchardt OHG, Germany) had a degree of hydrolysis ≥ 98% and molecular weight of approximately 60,000 g/mol. PVA hydrogels were prepared by dissolving the PVA polymer in distilled water with a particular weight composition. The solution was stirred and heated at temperatures of 70-90 °C to increase the solubility of the PVA polymer in water, as suggested in our previous study.[11] The mixture was perfectly dissolved, as indicated by a change in the form from liquid to paste. The mixture was placed in a mold to allow the freezing-thawing process to occur, in which the frozen mixture was kept at - 10 °C for 3 h, while thawing was performed at room temperature for 1 h. Various PVA hydrogel samples were prepared by using this freezing-thawing process from 1 to 6 times.

2.3. Fabrication of Magnetic Hydrogels

The magnetic hydrogels were fabricated by distributing the precipitate of magnetite nanoparticles into the hydrogel paste solution and then stirred to make uniform gels. The next steps were the freezing-thawing processes, similar to those used to prepare the PVA hydrogels. Various magnetic hydrogel samples were prepared by varying the concentration of the magnetite filler.

2.4. Characterization

2.4.1. X-ray Diffraction

Diffraction data measurement using an X-ray diffractometry Philips X-pert MPD was conducted in the angular positions (2θ) range from 15° to 65° with step size 0.02° using CuKα radiation (1.54 Å), voltage 40 kV, and current 30 mA to determine the phase and crystalline state of the PVA, PVA hydrogel and magnetic hydrogel samples. The magnetite samples were dried under vacuum at 100 °C for 1 h, and the PVA sample was crushed to form a homogeneous sample prior to X-ray diffraction measurements. Meanwhile, the PVA hydrogel and magnetic hydrogel samples were dried under vacuum at 37 °C for 48 h prior to X-ray diffraction measurements.

2.4.2. Small Angle X-ray Scattering (SAXS)

To analyze the size distribution of the original particles as defined by Zheng *et al*.[24] or primary particles, we used the SAXS instrument. This instrument is advantageous because it provides information concerning the size, morphology, inhomogeneities and interactions of nanopowders. Furthermore, the SAXS instrument provides nondestructive measurement and is able to measure the actual size of primary particles because the X-ray radiation from the SAXS instrument can be transmitted to the nanopowders sample; thus, this measurement technique is able to determine precisely the nanopowders size distributions.[24]

SAXS measurements were conducted at the Siam Photon Laboratory of Synchrotron Light Research Institute (SLRI), Thailand to observe the structural dimensions of the PVA hydrogels and magnetic hydrogels. The SAXS intensity, generated by an X-ray energy range of 6 to 9 keV, is presented as a function of the scattering vector, q, which is defined as $(4\pi/\lambda)\sin(\theta/2)$, where λ and θ are the wavelength of the X-rays and the scattering angle, respectively. The SAXS measurement used a CCD detector with a sample-to-detector distance (sdd) of 1,800 mm for the high q range and 4,500 mm for the low q range that covered the momentum transfer q range from 0.12 up to 2 nm^{-1}. The software SAXSIT was used to normalize, calibrate and correct the scattering intensities of the samples with the background.[25] The wavelength calibration was conducted by using Bragg reflections from silver behenate (AgBE). Data configurations that resulted from two different distances were extracted and merged by using SAXSIT [25] as well as analyzed by using the SASfit data analysis program.[26] For analyzing the data, the Beaucage and Teubner-Strey models were used because they are appropriate for calculating the average of the crystallite phases and the distance between crystallites of the PVA hydrogel. Moreover, two lognormal distribution was also utilized to obtain the primary particles, secondary particles, and clusters of the magnetic hydrogels.

2.4.3. Transmission Electron Microscopy (TEM)

Transmission Electron Microscope images were collected from a JEM1400 JEOL instrument to investigate the morphology of the magnetite nanoparticles.

2.4.4. Superconducting Quantum Interference Device (SQUID) Magnetometer

The magnetic properties of the magnetite nanoparticles and the magnetic hydrogels were taken at the Department of Basic Science, Graduate School of Arts and Sciences, the University of Tokyo by using a SQUID (Quantum Design, MPMS-5S) magnetometer. Magnetization curves of the samples were constructed after obtaining the magnetization values at room temperature as a function of the applied magnetic field between - 5 and 5 T.

3. Results and Discussion

3.1. X-Ray Diffractions Characterization

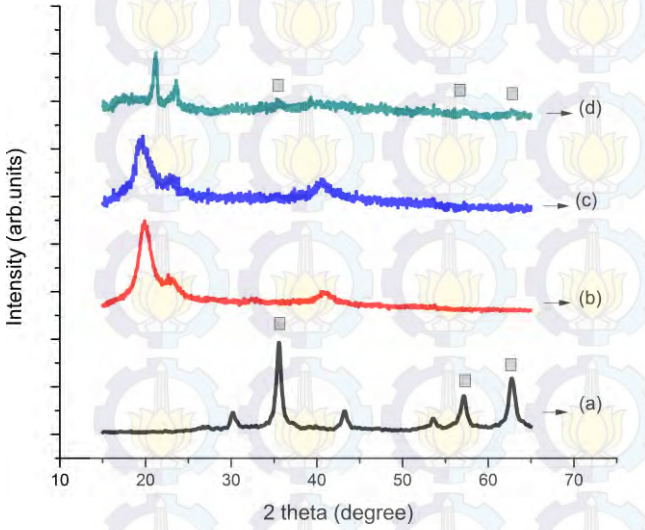

Fig. 1. X-ray diffraction patterns of magnetite nanoparticles (a), PVA (b), hydrogel (c) and magnetic hydrogel (d). The square marks represent the diffraction peaks from the magnetite.

The X-ray diffraction patterns of the magnetite powder, PVA, hydrogel and magnetic hydrogel are shown in Figs. 1a, b, c, and d, respectively. We confirm that the powder contains only cubic magnetite Fe_3O_4 (PDF No. 65-3107) with an estimated crystallite size of approximately 12 nm, as suggested by our earlier technique.[27]

The XRD patterns of the PVA and hydrogel are in good agreement with that previously reported.[13,28] The XRD pattern of the magnetic hydrogel (Fig. 1d) indicates the presence of magnetite in the hydrogel.

3.2. SAXS Characterization

Fig. 2 shows the SAXS patterns of the PVA hydrogels with different numbers of F-T cycles. The calculation model used to analyze the PVA hydrogels sample is a combination between the Teubner-Strey and Beaucage models. The Teubner-Strey model, which explains a quasi-periodic repeat distance (d) and correlation length (ξ), displays a scattering intensity as follows.[26,29]

$$I(q) = \frac{8\pi\langle\eta^2\rangle\xi}{a^2 - 2bq^2 + q^4} \quad (1)$$

where η^2 is the squared scattering length density contrast, a is a positive quantity,

$$a = k^2 + \frac{1}{\xi^2} \quad (2)$$

and b can be positive or negative depending on the relative magnitude of the wave vector $k = 2\pi/d$ and ξ.

$$b = k^2 - \frac{1}{\xi^2} \quad (3)$$

Meanwhile, the Beaucage model[26,30] was used to determine the dimensional structure from the samples as follows.

$$I(q) = G\exp(-q^2 R_g{}^2/3) + B\left[erf(qR_g/\sqrt{6})\right]^{3P}/q^P \quad (4)$$

where R_g is the gyration radius of a structure, P is a characteristic of the fractal dimension, G is the Guinier pre-factor of the larger structure, B is a pre-factor specific to the type of power-law scattering and the $[erf(qR_g/\sqrt{6})]^{3P}$ term is a smooth transition between the two regions. From equations (1) to (4), the d and ξ variables were refined by using the SASfit software to reveal a quasi-periodic repeat distance and correlation length of the PVA hydrogel samples.

The correlation length (ξ) values of the PVA hydrogels as a function of the number of F-T cycles are shown in Table 1, where they decrease slightly from cycle 1 to 3 and are relatively stable from cycle 4 to 6. Therefore, 3-cycle F-T treatment can be considered as effective to process the PVA hydrogel with good chain mobility. PVA chain mobility and crystallite average size (the correlation length) are important factors to organize solute movement within the PVA hydrogel. Reduction of the crystallite average

size will have an effect on the movement of the solute within the PVA hydrogel, such as the enhancement of polymer chain mobility that caused the PVA hydrogel to be more flexible. In contrast, the quasi-periodic repeat distances of the PVA hydrogels do not significantly change with the number of F-T cycles. These results show that the crystallite PVA is more dominant than the amorphous one.

According to the Table 1, the average correlation length (ξ) of the PVA hydrogels is approximately 3.9 nm, while the average distance between crystallites (d) is approximately 18 nm. These findings allow us to construct a structure building as schematically illustrated in Fig. 3, which is similar to previous reports by Puspitasari *et al.*[15] and Millon *et al.*.[16] They found that the PVA hydrogels consisted of polymer crystallites with a radius of approximately 3 nm and an average distance between polymer crystallites of 15-19 nm. With these results, we suggest that the size of the polymer-rich domain in this work is more than 80 nm in diameter, as also claimed by Puspitasari *et al.*.[15] Furthermore, the ξ and d values in this work are also consistent with those reported by Ricciardi *et al.*.[31] They concluded that the PVA hydrogel consisted of two regions, namely, polymer-rich and polymer-poor regions. The polymer-rich regions were composed of amorphous regions of approximately 15-30 nm and crystallites, whereas the polymer-poor regions have dimensions of more than 100 nm.

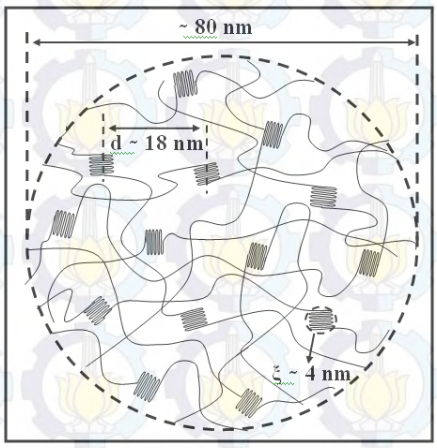

Fig. 3. The schematic illustration of PVA hydrogels with an average of the crystallite phases of approximately 4 nm and an average distance between crystallites of approximately 18 nm. The size of the polymer-rich phase is more than 80 nm, as suggested by Puspitasari *et al.*.[15]

Table 1. Parameters of crystallites and quasi-periodic repeat distance for PVA hydrogels.

Number of F-T process	ξ (nm)	d (nm)
1	4.1	18
2	3.9	19
3	3.8	18
4	3.9	18
5	3.9	19
6	3.9	18

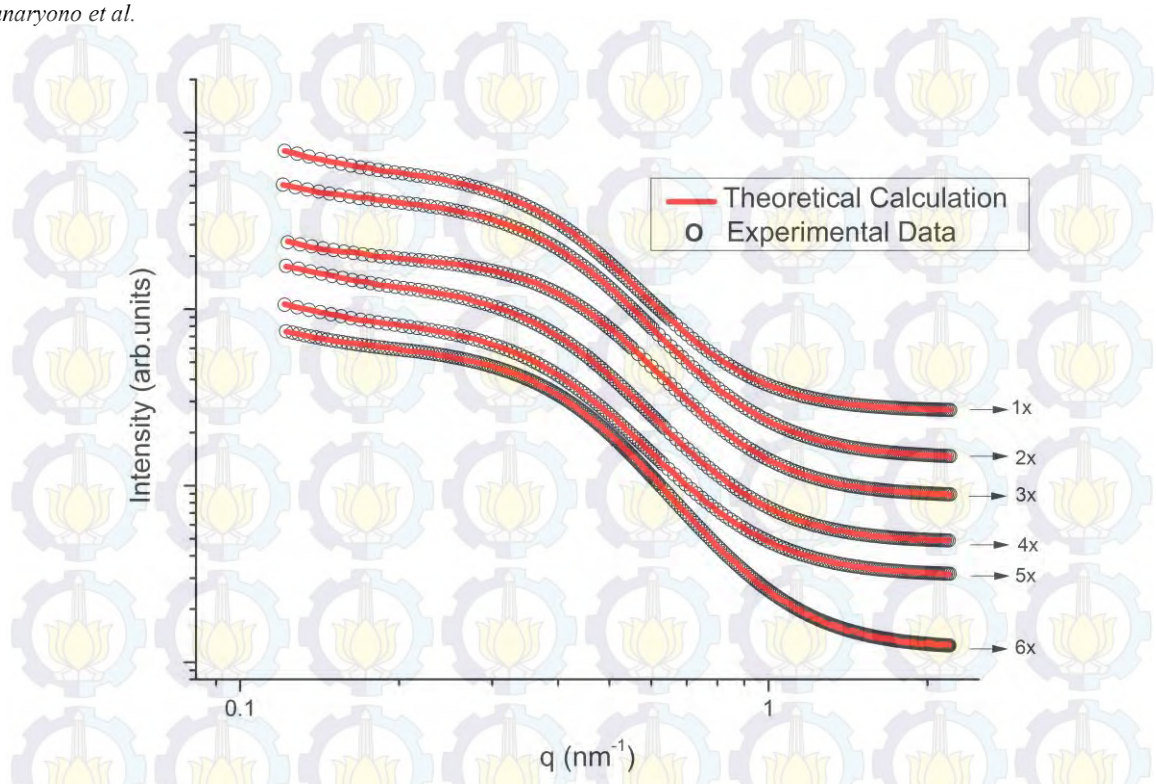

Fig. 2. SAXS patterns of hydrogels with the number of F-T cycles of: 1×, 2×, 3×, 4×, 5×, and 6×. The calculated fitting lines were constructed by using Eqs. (1)-(4) embedded in the SASfit software. Note that due to similarity in absolute values, the intensity scale is s lightly stretched to allow for better pattern viewing.

The secondary particles of the magnetite nanoparticles are a general phenomenon that occurs in nanopowders due to the strong interactions between magnetic particles. These secondary particles are structured by primary particles as a consequence of their aggregation. The finite cluster size is a compound of primary and secondary particles in magnetic hydrogel, which might be due to the interactions among nanoparticles as well as between nanoparticles and the PVA hydrogel. In this work, the diameter of the clusters is represented by the length correlation of the mass fractal from the nanoparticles magnetite in the magnetic hydrogel.

Additionally, a lognormal distribution function has been applied to explore the size distribution of the magnetite nanoparticles before and after immersion as in the magnetic hydrogels. The function is as previously given.[26,32]

$$N(r) = \frac{1}{r\sigma\sqrt{2\pi}} exp\left(-\frac{1}{2}\left[\frac{ln(r/r_o)}{\sigma} \right]^2 \right) \quad (5)$$

where σ is a scale or width parameter and r_o is the radius gyration of the primary particles.

Furthermore, the scattering intensity function *I(q)* of *N* nanoparticles of magnetite per unit volume is written as[33]

$$I(q) \propto \frac{d\Sigma}{d\Omega} = N_p P(q) S(q) + \text{bkg} \quad (6)$$

or, over all covered scattering space, can be expressed as,

$$I(q) \propto \int_0^\infty N_p(r) F_N^{\,2}(q,r) S(q,\varsigma,D,r) dr \quad (7)$$

where ‘‘bkg’’ is the incoherent background, $N_p(r)$ is the number density of the primary particles, $P(q)$ is the form factor, $F(q,r)$ is the scattering amplitude and $S(q,\varsigma,D,r)$ is the structure factor. For a fractal object, the structure factor $S(q,\varsigma,D,r)$ represents the interaction between particles and can be determined via the density autocorrelation function of the clusters $g(\varsigma,D,r)$, where

$$g(\varsigma,D,r) \propto r^{D-d} \exp(-r/\varsigma) \quad (8)$$

as suggested by Teixeira,[34] while structure factors are given by

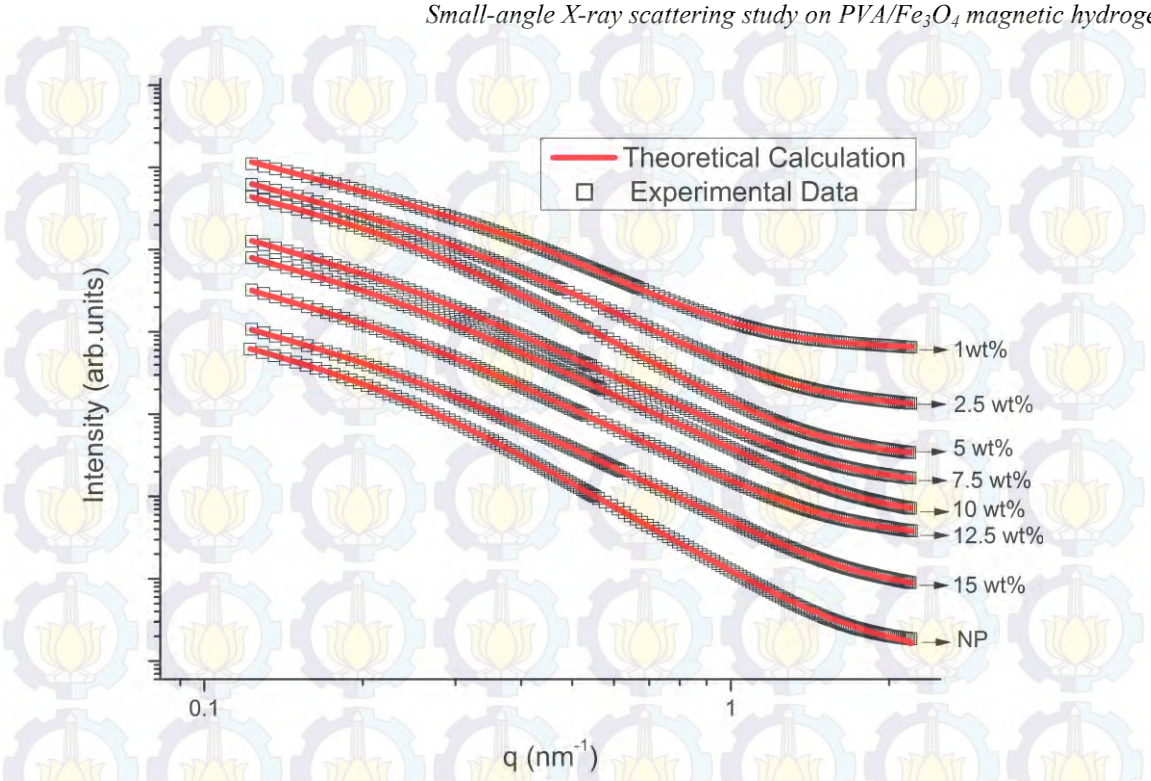

Fig. 4. SAXS pattern of magnetite nanoparticles (NP) and magnetic hydrogel with a filler of magnetite content of: 1 wt%, 2.5 wt%, 5 wt%, 7.5 wt%, 10 wt%, 12.5 wt%, and 15 wt%. Note also the stretched vertical scale to allow for better pattern viewing.

$$S(q,\varsigma,D,r) = 1 + \frac{D\Gamma(D-1)\sin([D-1]\arctan(q\varsigma))}{(qr_0)^D\left[1+(q\varsigma)^{-2}\right]^{(D-1)/2}} \tag{9}$$

where d is the spatial dimension, $\Gamma(r)$ is the gamma function, and ς is the diameter of the clusters.

In this study, we assume that the magnetite nanoparticles are spherical. The data of the magnetite nanoparticles (Fig. 4) was fitted by using the two-lognormal distribution functions of Eq. (7) for a single structure factor, which is written as follows[35]

$$I(q) \propto \int_0^\infty N_1(r_1)F_N^{\,2}(q,r_1)S(q,\varsigma,D,r_1)dr_1 + \int_0^\infty N_2(r_2)F_N^{\,2}(q,r_2)S(q,\varsigma,D,r_2)dr_2 \tag{10}$$

where r_1 represents the radius of the primary particle and r_2 represents the radius of the secondary particle. The variables r, ς, and D from equation (9) to (10) were refined by using the SASfit software to expose the radius gyration of the primary particles, secondary particles, and diameter of the clusters as well as the fractal dimensions of the magnetic hydrogel samples. The simultaneous use of these two functions in the fitting procedure leads to the term "global fitting".

The analysis results showed that the size distributions of magnetite nanoparticles consist of primary and secondary particles with a diameter of 3.2 nm and 9.6 nm, respectively, which is similar to that reported by Yusuf *et al.*.[35] They found that the diameters of nanoparticles are ~ 1.2 and 4.1 nm when using the two lognormal distribution analyses. In other study, the magnetite nanoparticles had primary particles constructing clusters in 3 dimension as secondary particles analyzed by small angle neutron scattering (SANS).[21] Accordingly, in this study, we claim that the natural clusters of magnetite are composed of magnetite primary particle clusters. The diameter of the secondary particles for these magnetite nanoparticles was confirmed by a TEM image, which showed an average particle diameter of 9-12 nm. This result is reasonably close to the XRD crystallite size of the magnetite nanoparticles of 8.9-12.5 nm in this experiment. The morphology of the magnetite nanoparticle (Fig. 5) is irregular and tends to cluster. Magnetite nanoparticles form natural clusters due to the strong pull force from one particle to the other particles. A similar conclusion was provided by Girod

et al.,[36] who used laboratory SAXS at the BAMline and reported that the diameters of primary particles were ~ 2 nm (of magnetite and maghemite phases) after a synthesis at room temperature and ~ 7 nm after a synthesis at 80 °C (of solely maghemite phase). The diameter of primary particles in this paper has a similar value to their work, where in both reports, a process at room temperature has been introduced.

Table 2. Parameters of the size distribution of magnetite nanoparticles in magnetic hydrogels resulting from applying the global fitting procedure using Eqs. (9)–(10) to the synchrotron SAXS data. Referring to Eqs. (5)-(10), r_1 is the radius of the primary particle, r_2 is the radius of the secondary particles and ς is the average diameter of the clusters. These parameters were adjusted during the fitting.

Sample	r_1 (nm)	r_2 (nm)	ς (nm)	D
1 wt%	1.6	3.2	12.8	2.5
2.5 wt%	1.6	3.3	18.9	2.3
5 wt%	1.6	3.4	21.9	2.2
7.5 wt%	1.6	3.6	23.1	2.2
10 wt%	1.6	3.9	25.6	2.2
12.5 wt%	1.6	4.0	28.0	2.2
15 wt%	1.6	4.1	30.4	2.2
NP	1.6	4.8	34.8	2.4

The diameter of the primary particles of the magnetite nanoparticles (~ 3 nm), which was derived by using the synchrotron radiation SAXS technique, is lower than the XRD-derived crystallite size (~ 12 nm), which is evidently similar to the diameter of the secondary particles. This result is similar to the data reported by Hernandez *et al.*.[17] They showed that the diameter of primary particles of iron oxide nanoparticles (NPs) synthesized in an alginate solution (Alg-FF) is 3.6 nm by using SAXS data and the Scherrer derived crystal size is 6.7 nm by using WAXD. This is because the electron density between the magnetite nanoparticles and their environment is different. With this condition, primary particles tend to form secondary particles, and every primary particle in the secondary particles has the potential to scatter a beam of a small angle.[24] The SAXS technique shows the actual size of the primary particles caused by the transmission of each nanoparticle (primary particle), whereas X-ray diffraction reveals the crystal orientation of the magnetite, which is compiled by the reflection of each crystalline of the nanoparticles. The crystal orientation of the nanoparticles can be structured by one or more of the primary particles.

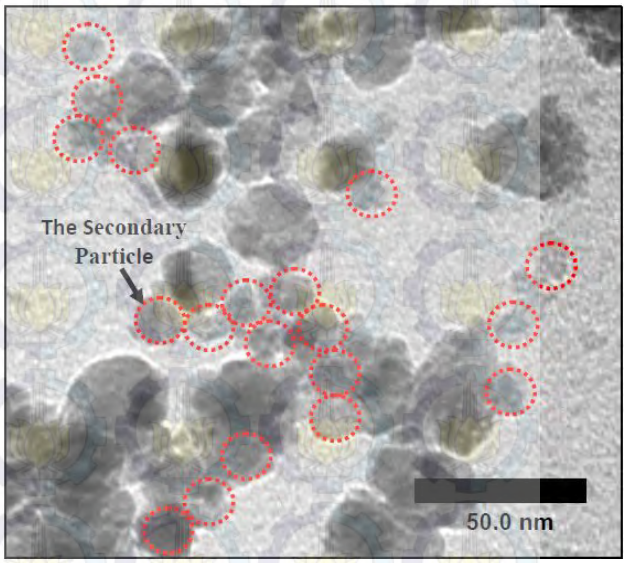

Fig. 5. TEM image of magnetite nanoparticles.

On the other hand, the scattering intensities of the magnetite nanoparticles in the matrix of the PVA polymer are more dominant than the crystallites of the PVA hydrogels. Therefore, the scattering intensity of a magnetic hydrogel is a representation of the filler of the magnetite nanoparticles. To analyze the distribution of the magnetite filler in the magnetic hydrogel, a two-lognormal distribution analysis was again applied by using Eqs. (9)-(10). As shown in Table 2, all samples exhibit a clustering phenomenon of the magnetite nanoparticles in the PVA hydrogel matrices. Two facts can be drawn from the table, i.e., (1) the secondary particles of the magnetite nanoparticles compose a mass fractal structure and (2) the size of the clusters of the magnetite are significantly reduced from 30.4 to 12.8 nm with decreasing concentration of the magnetite nanoparticles. A schematic illustration of the distribution of the magnetite nanoparticles in the magnetic hydrogels is presented in Fig. 6.

Based on Eqs. (7) and (8), the scattering function is proportional to the density of an autocorrelation function of the clusters. Meanwhile, the autocorrelation function of fractal clusters is proportional to the size of the aggregate. The results in Table 2 confirm that the higher the concentration of the magnetite filler in the magnetic hydrogels, the higher the density autocorrelation function of the clusters and the diameter of the clusters. It can be concluded that the filler of the magnetite nanoparticles

is composed of mass fractal clusters in the matrix of the PVA hydrogels. The diameter of the clusters of the magnetite nanoparticles in the PVA hydrogels declines significantly as the content of the magnetite nanoparticles decreases. It can be concluded that the matrix of the PVA hydrogels is effective at reducing the diameter of the clusters of the magnetite nanoparticles.

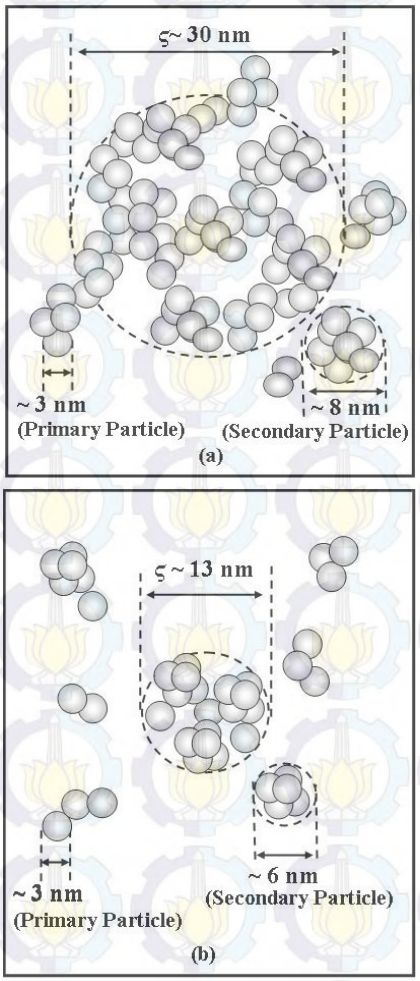

Fig. 6. The schematic illustration of the distribution of magnetite nanoparticles in magnetic hydrogels with a filler of (a) 15 wt% and (b) 1 wt% of magnetite.

3.3. SQUID Pattern of Magnetite Nanoparticles and Magnetic Hydrogels

Fig. 7 provides the magnetization hysteresis curve of the magnetic hydrogels and the magnetite nanoparticles (as shown in the insert picture). The magnetization curve for the magnetite nanoparticles shows that the values of coercivity force is approximately negligible pointing out superparamagnetic behavior.[37,38] Another experiment showed that the diameter of primary particles of magnetite in range of 7 to 9 nm which is larger than that of this experimental result (3 nm) also presenting superparamagnetic behavior.[39,40]

The curves show that the saturation magnetization (M_s) value are 34.67, 6.52, and 0.37 emu/g for magnetite nanoparticles and 15%, and 1% magnetic hydrogels, respectively. The 1% magnetic hydrogel has the lowest magnetic response as a consequence of having the lowest magnetite nanoparticles content, diameter of secondary particles as well as clusters. The lower magnetite nanoparticles concentration that followed by the increasing particles free volume and the decreasing the interaction energy between magnetite nanoparticles in hydrogel magnetic affected the poorer magnetic-sensitive behavior.[4] The diameter of the secondary particles and clusters of magnetite in the 15% and 1% magnetic hydrogels dropped from 9.2 to 6.4 nm and 30.4 to 12.8 nm, respectively, which was followed by a decrease in the saturation magnetization from 6.52 to 0.37 emu/g. This result agrees with previous report by Yoon *et al.*[8] for magnetite nanoparticles. They stated that the saturation magnetization of magnetite nanoparticles decrease from 78 to 53 emu/g when the clusters of magnetite nanoparticles decrease from 42 to 35 nm. The smaller of the particles size, the smaller a portion of the particle volume contributed in the effective magnetic volume and the saturation magnetization decreases due to the effect of surface.

Furthermore, the magnetization magnetic hydrogels containing 15% and 1% of magnetite increased slightly, approximately ~25% and ~ 5% from the expected values of 5.20 and 0.35 emu/g, respectively. This phenomenon is a consequence of the presence of different clustering of magnetite in the magnetic hydrogel magnetic. The low value of saturation magnetization is believed to be due to the existence of the PVA matrix in magnetic hydrogel, which simply limits the magnetic effect from the magnetite nanoparticles. It appears that the magnetization is proportional to the magnetite content in the PVA hydrogel and its clustering. The lower the magnetite content, the smaller the secondary particle and cluster diameters.

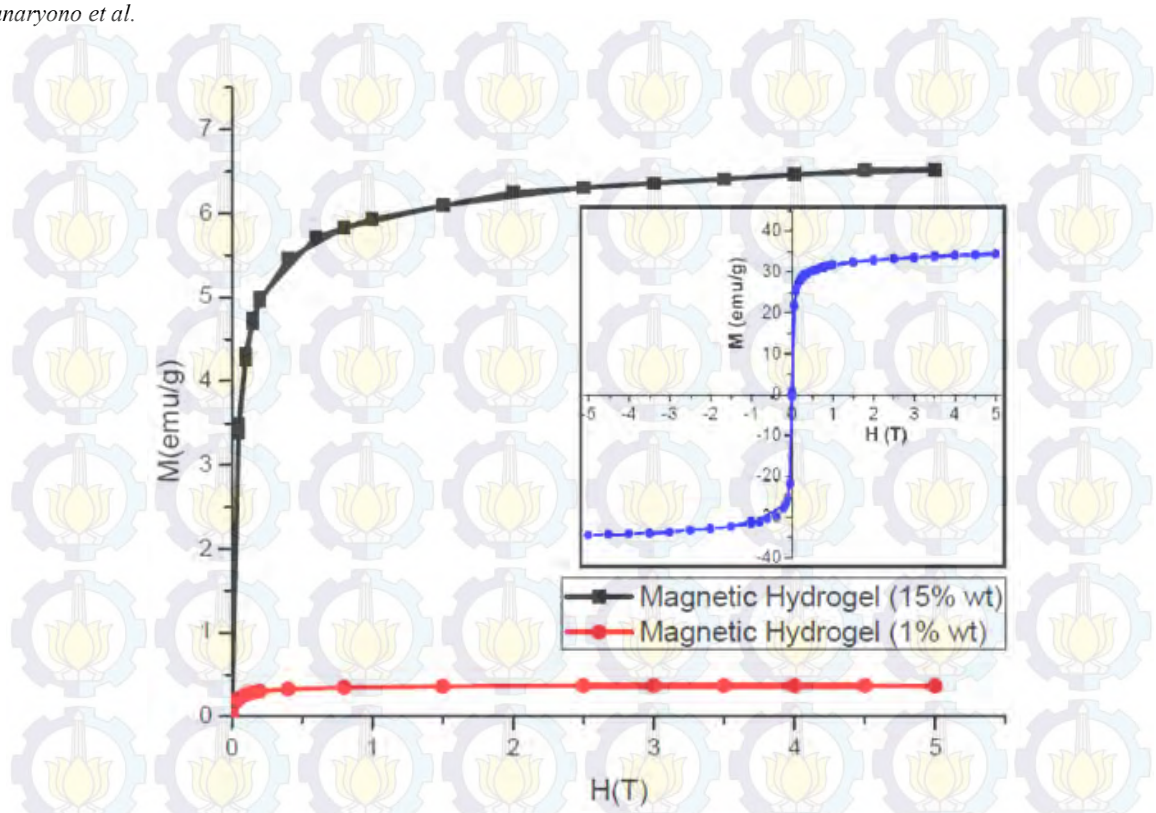

Fig. 7. SQUID patterns of magnetite nanoparticles, magnetic hydrogel (15 wt%), and (1 wt%). The insert picture is the SQUID patterns for the magnetite.

4. Conclusion

A synchrotron SAXS analysis has been used to confirm the structural dimensions of PVA hydrogels and magnetic hydrogel. The Beaucage and Teubner-Strey calculation models are well-fitted with the small-angle scattering data to give the average structural dimensions of PVA hydrogels, i.e., 3.9 nm (crystallites), with an average distance between crystallites of approximately 18 nm. The secondary particles and clusters of magnetite nanoparticles in the magnetic hydrogels analyzed by two lognormal distribution functions exhibit the significant clustering degradation from 30.4 to 12.8 nm and 9.6 to 6.4 nm respectively with decreasing the magnetite nanoparticles content. Moreover, the magnetite nanoparticles and magnetic hydrogels (1 and 15 wt% magnetite) associates with the superparamagnetic characteristic. The saturation magnetization of the magnetic hydrogels, being proportional to the magnetite content in the PVA hydrogel and its clustering, declined with decreasing diameter of the secondary particles and clusters of the magnetite.

Acknowledgments

This research was partially supported by Hibah Kompetensi, DP2M (2013 – 2015), and PPPKI program 2013, DIKTI, Kemendikbud. The authors are grateful to Riken and The University of Tokyo, Japan for the beam time of SQUID measurements in 2013. The authors are also grateful to the Synchrotron Light Research Institute (SLRI), Thailand for the beam time proposal with ID No. 1498 in 2014.

References

1. E.-R. Kenawy, E. A. Kamoun, M. S. Mohy Eldin, and M. A. El-Meligy, "Physically crosslinked poly(vinyl alcohol)-hydroxyethyl starch blend hydrogel membranes: Synthesis and characterization for biomedical applications," *Arab. J. Chem.*, vol. 7, no. 3, pp. 372–380, Jul. 2014.
2. H. Priya James, R. John, A. Alex, and K. R. Anoop, "Smart polymers for the controlled delivery of drugs – a concise overview," *Acta Pharm. Sin. B*, vol. 4, no. 2, pp. 120–127, Apr. 2014.
3. Y. Osada, J. Ping Gong, and Y. Tanaka, "Polymer Gels," *J. Macromol. Sci. Part C*, vol. 44, no. 1, pp. 87–112, Dec. 2004.

4. T.-Y. Liu, S.-H. Hu, K.-H. Liu, D.-M. Liu, and S.-Y. Chen, "Study on controlled drug permeation of magnetic-sensitive ferrogels: Effect of Fe_3O_4 and PVA," *J. Controlled Release*, vol. 126, no. 3, pp. 228–236, Mar. 2008.
5. L. L. Lao and R. V. Ramanujan, "Magnetic and hydrogel composite materials for hyperthermia applications.," *J. Mater. Sci. Mater. Med.*, vol. 15, no. 10, pp. 1061–1064, Oct. 2004.
6. P. An, F. Zuo, X. Li, Y. Wu, J. Zhang, Z. Zheng, X. Ding, and Y. Peng, "A Bio-Inspired Polydopamine Approach to Preparation of Gold-Coated Fe_3O_4 Core–Shell Nanoparticles: Synthesis, Characterization and Mechanism," *Nano*, vol. 08, no. 06, p. 1350061, 2013.
7. Z. Varga, G. Filipcsei, and M. Zrínyi, "Magnetic field sensitive functional elastomers with tuneable elastic modulus," *Polymer*, vol. 47, no. 1, pp. 227–233, Jan. 2006.
8. K. Y. Yoon, M. Mehrmohammadi, A. Borwankar, S. Y. Emelianov, and K. P. Johnston, "Synthesis of Iron Oxide Nanoclusters with Enhanced Magnetization and Their Applications in Pulsed Magneto-Motive Ultrasound Imaging," *Nano*, vol. 10, no. 05, p. 1550073, 2015.
9. N. Sahiner, S. Butun, and P. Ilgin, "Soft hydrogel particles with high functional value," *Colloids Surf. Physicochem. Eng. Asp.*, vol. 381, no. 1–3, pp. 74–84, May 2011.
10. W. H. Li, X. Z. Zhang, and H. Du, "Magnetorheological Elastomers and Their Applications," in *Advances in Elastomers I*, vol. 11, P. M. Visakh, S. Thomas, A. K. Chandra, and A. P. Mathew, Eds. Springer Berlin Heidelberg, 2013, pp. 357–374.
11. Sunaryono, A. Taufiq, Munaji, B. Indarto, Triwikantoro, M. Zainuri, and Darminto, "Magneto-elasticity in hydrogels containing Fe_3O_4 nanoparticles and their potential applications," *AIP Conf. Proc.*, vol. 1555, no. 1, pp. 53–56, 2013.
12. R. V. Ramanujan and L. L. Lao, "The mechanical behavior of smart magnet–hydrogel composites," *Smart Mater. Struct.*, vol. 15, no. 4, p. 952, 2006.
13. P. J. Reséndiz-Hernández, O. S. Rodríguez-Fernández, and L. A. García-Cerda, "Synthesis of poly(vinyl alcohol)–magnetite ferrogel obtained by freezing–thawing technique," *VIII Lat. Am. Workshop Magn. Magn. Mater. Their Appl.*, vol. 320, no. 14, pp. e373–e376, Jul. 2008.
14. J. Gonzalez, C. Hoppe, D. Muraca, F. Sánchez, and V. Alvarez, "Synthesis and characterization of PVA ferrogels obtained through a one-pot freezing–thawing procedure," *Colloid Polym. Sci.*, vol. 289, no. 17–18, pp. 1839–1846, 2011.
15. T. Puspitasari, K. M. L. Raja, D. S. Pangerteni, A. Patriati, and E. G. R. Putra, "Structural Organization of Poly(vinyl alcohol) Hydrogels Obtained by Freezing/Thawing and γ-Irradiation Processes: A Small-Angle Neutron Scattering (SANS) Study," *Int. Conf. Innov. Polym. Sci. Technol.*, vol. 4, no. 0, pp. 186–193, 2012.
16. L. E. Millon, M.-P. Nieh, J. L. Hutter, and W. Wan, "SANS Characterization of an Anisotropic Poly(vinyl alcohol) Hydrogel with Vascular Applications," *Macromolecules*, vol. 40, no. 10, pp. 3655–3662, May 2007.
17. R. Hernandez, J. Sacristan, A. Nogales, T. A. Ezquerra, and C. Mijangos, "Structural organization of iron oxide nanoparticles synthesized inside hybrid polymer gels derived from alginate studied with small-angle X-ray scattering.," *Langmuir ACS J. Surf. Colloids*, vol. 25, no. 22, pp. 13212–13218, Nov. 2009.
18. A. Priola, A. D. Gianni, R. Bongiovanni, S. G. Starodubtsev, S. S. Abramchuck, S. N. Polyakov, V. V. Volkov, E. V. Schtykova, and K. A. Dembo, "Effect of the swelling degree on the formation of magnetite nanoparticles in hydrogels," *Eur. Polym. J.*, vol. 46, no. 11, pp. 2105–2111, Nov. 2010.
19. O. Moscoso-Londono, J. S. Gonzalez, D. Muraca, C. E. Hoppe, V. A. Alvarez, A. Lopez-Quintela, L. M. Socolovsky, and K. R. Pirota, "Structural and magnetic behavior of ferrogels obtained by freezing thawing of polyvinyl alcohol/ poly(acrylic acid) (PAA)-coated iron oxide nanoparticles," *Eur. Polym. J.*, vol. 49, no. 2, pp. 279–289, Feb. 2013.
20. R. Hernandez, J. Sacristan, A. Nogales, M. Fernandez, T. A. Ezquerra, and C. Mijangos, "Structure and viscoelastic properties of hybrid ferrogels with iron oxide nanoparticles synthesized in situ," *Soft Matter*, vol. 6, no. 16, pp. 3910–3917, 2010.
21. A. Taufiq, Sunaryono, E. Rachman Putra, A. Okazawa, I. Watanabe, N. Kojima, S. Pratapa, and Darminto, "Nanoscale Clustering and Magnetic Properties of $Mn_xFe_{3-x}O_4$ Particles Prepared from Natural Magnetite," *J. Supercond. Nov. Magn.*, vol. 28, no. 9, pp. 2855–2863, 2015.
22. Sunaryono, A. Taufiq, Mashuri, S. Pratapa, M. Zainuri, Triwikantoro, and Darminto, "Various Magnetic Properties of Magnetite Nanoparticles Synthesized from Iron-sands by Coprecipitation Method at Room Temperature," *Trans Tech Publ. Switz.*, vol. 827, pp. 229–234, Apr. 2015.
23. A. Taufiq, Sunaryono, E. Giri Rachman Putra, S. Pratapa, and Darminto, "Nano-structural studies on Fe_3O_4 particles dispersing in a magnetic fluid using X-ray diffractometry and small-angle neutron scattering," *Trans Tech Publ. Switz.*, vol. 827, pp. 213–218, Apr. 2015.
24. Y. Zheng, S. Huang, and L. Wang, "Distribution Analysis of Nanoparticle Size by Small Angle X-ray Scattering," *Avestia Publ.*, vol. I, no. I, pp. 124–132, 2012.
25. S. Rugmai and S. Soontaranon, *Manual for SAXS/WAXS data processing using SAXSIT*. 2013.

26. J. Kohlbrecher, *User guide for the SASfit software package*. Paul Scherrer Institute Laboratory for Neutron Scattering (LNS) CH-5232 Villigen PSI joachim.kohlbrecher@psi.ch, 2012.
27. S. Pratapa, L. Susanti, Y. A. S. Insany, Z. Alfiati, B. Hartono, Mashuri, A. Taufiq, A. Fuad, Triwikantoro, M. A. Baqiya, S. Purwaningsih, E. Yahya, and Darminto, "XRD line-broadening characteristics of M-oxides (M = Mg, Mg-Al, Y, Fe) nanoparticles produced by coprecipitation method," *AIP Conf. Proc.*, vol. 1284, no. 1, pp. 125–128, 2010.
28. L. A. García-Cerda, M. U. Escareño-Castro, and M. Salazar-Zertuche, "Preparation and characterization of polyvinyl alcohol–cobalt ferrite nanocomposites," *Non-Cryst. Solids 8 Proc. 8th Int. Workshop Non-Cryst. Solids 8th Int. Workshop Non-Cryst. Solids*, vol. 353, no. 8–10, pp. 808–810, Apr. 2007.
29. M. Teubner and R. Strey, "Origin of the scattering peak in microemulsions," *J. Chem. Phys.*, vol. 87, no. 5, pp. 3195–3200, 1987.
30. G. Beaucage, "Approximations Leading to a Unified Exponential/Power-Law Approach to Small-Angle Scattering," *J. Appl. Crystallogr.*, vol. 28, no. 6, pp. 717–728, 1995.
31. R. Ricciardi, G. Mangiapia, F. Lo Celso, L. Paduano, R. Triolo, F. Auriemma, C. De Rosa, and F. Lauprêtre, "Structural Organization of Poly(vinyl alcohol) Hydrogels Obtained by Freezing and Thawing Techniques: A SANS Study," *Chem. Mater.*, vol. 17, no. 5, pp. 1183–1189, Mar. 2005.
32. C. M. Sorensen and G. M. Wang, "Size distribution effect on the power law regime of the structure factor of fractal aggregates," *Phys Rev E*, vol. 60, no. 6, pp. 7143–7148, Dec. 1999.
33. M. F. van Raap, P. M. Zélis, D. Coral, T. Torres, C. Marquina, G. Goya, and F. Sánchez, "Self organization in oleic acid-coated $CoFe_2O_4$ colloids: a SAXS study," *J. Nanoparticle Res.*, vol. 14, no. 9, pp. 1–10, 2012.
34. J. Teixeira, "Small-angle scattering by fractal systems," *J. Appl. Crystallogr.*, vol. 21, no. 6, pp. 781–785, 1988.
35. S. M. Yusuf, M. D. Mukadam, J. M. De Teresa, M. R. Ibarra, J. Kohlbrecher, A. Heinemann, and A. Wiedenmann, "Structural and magnetic properties of amorphous iron oxide," *Phys. B Condens. Matter*, vol. 405, no. 4, pp. 1202–1206, Feb. 2010.
36. M. Girod, S. Vogel, W. Szczerba, and A. F. Thünemann, "How temperature determines formation of maghemite nanoparticles," *10th Int. Conf. Sci. Clin. Appl. Magn. Carr. 10-14 June 2014 Dresd. Ger.*, vol. 380, no. 0, pp. 163–167, Apr. 2015.
37. R. Rameshbabu, R. Ramesh, S. Kanagesan, A. Karthigeyan, and S. Ponnusamy, "Synthesis and Study of Structural, Morphological and Magnetic Properties of $ZnFe_2O_4$ Nanoparticles," *J. Supercond. Nov. Magn.*, vol. 27, no. 6, pp. 1499–1502, Jun. 2014.
38. K. S. Sivudu and K. Y. Rhee, "Preparation and characterization of pH-responsive hydrogel magnetite nanocomposite," *Colloids Surf. Physicochem. Eng. Asp.*, vol. 349, no. 1–3, pp. 29 – 34, 2009.
39. P. Saravanan, S. Alam, L. D. Kandpal, and G. N. Mathur, "Effect of substitution of Mn ion on magnetic properties of Fe_3O_4 nanocrystallites," *J. Mater. Sci. Lett.*, vol. 21, no. 14, pp. 1135–1137, Jul. 2002.
40. W. Cai and J. Wan, "Facile synthesis of superparamagnetic magnetite nanoparticles in liquid polyols," *J. Colloid Interface Sci.*, vol. 305, no. 2, pp. 366–370, Jan. 2007.